

TCP-Diffusion: A Multi-modal Diffusion Model for Global Tropical Cyclone Precipitation Forecasting with Change Awareness

Cheng Huang^{1,2}, Pan Mu¹, Cong Bai^{1*}, Peter AG Watson²

¹College of Computer Science, Zhejiang University of Technology

²School of Geographical Sciences, University of Bristol

Abstract

Precipitation from tropical cyclones (TCs) can cause disasters such as flooding, mudslides, and landslides. Predicting such precipitation in advance is crucial, giving people time to prepare and defend against these precipitation-induced disasters. Developing deep learning (DL) rainfall prediction methods offers a new way to predict potential disasters. However, one problem is that most existing methods suffer from cumulative errors and lack physical consistency. Second, these methods overlook the importance of meteorological factors in TC rainfall and their integration with the numerical weather prediction (NWP) model. Therefore, we propose Tropical Cyclone Precipitation Diffusion (TCP-Diffusion), a multi-modal model for global tropical cyclone precipitation forecasting. It forecasts TC rainfall around the TC center for the next 12 hours at 3 hourly resolution based on past rainfall observations and multi-modal environmental variables. Adjacent residual prediction (ARP) changes the training target from the absolute rainfall value to the rainfall trend and gives our model the capability of rainfall change awareness, reducing cumulative errors and ensuring physical consistency. Considering the influence of TC-related meteorological factors and the useful information from NWP model forecasts, we propose a multi-model framework with specialized encoders to extract richer information from environmental variables and results provided by NWP models. The results of extensive experiments show that our method outperforms other DL methods and the NWP method from the European Centre for Medium-Range Weather Forecasts (ECMWF).

Introduction

Tropical cyclone (TC) precipitation refers to the substantial rainfall events that accompany the formation, development, and movement of tropical cyclones. These precipitation events can lead to severe disasters in the affected regions, like heavy rainfall, flooding, mudslides, and landslides. These TC rainfall-related disasters cause more economic losses and deaths than strong winds (Wendler-Bosco and Nicholson 2022), yet most TC forecasting efforts focus only on track and wind intensity. Therefore, it is important to accurately predict the precipitation around the TC center.

Numerical weather prediction (NWP) is widely used for various weather forecasting tasks, including TC forecasting. It simulates atmospheric dynamics, thermodynamics, and

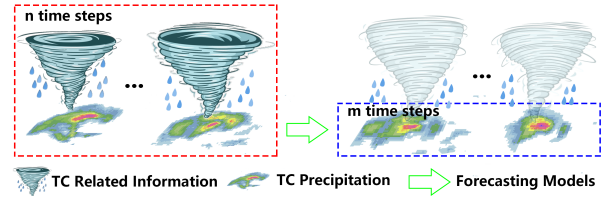


Figure 1: The TC precipitation forecasting task. The red box represents historical data, which is considered to be the input of the forecasting model. The blue box represents the TC rainfall that should be predicted. This paper just focuses on the prediction of TC rainfall.

physical processes by solving the physical and mathematical equations that describe changes in wind, temperature, humidity, and pressure (Bai et al. 2020). It has achieved impressive results, but the development in NWP research has been gradual (Benjamin et al. 2018). Additionally, not all physical mechanisms of TCs are fully understood, which prevents the formulation of perfect physical and mathematical equations for NWP (Xu et al. 2024). Furthermore, NWP typically runs on supercomputer platforms, consuming extensive computational resources and time for predictions, when predicting a high-resolution result. Nonlinear simulation also poses a significant challenge for NWP. Fortunately, the development of deep learning (DL) offers solutions to these NWP challenges. DL-based methods excel at modeling nonlinear processes, and the cost of model training and inference is relatively low, requiring only a few graphics processing units (GPUs) for regular AI tasks.

DL methods have been applied to many meteorological tasks, like TC track and intensity prediction (Huang et al. 2022, 2023), TC rainfall downscaling (Vosper et al. 2023), global meteorological variable prediction (Bi et al. 2023; Lam et al. 2023), and precipitation nowcasting (Bai et al. 2022). For precipitation nowcasting, several works have used DL since 2013. Initially, researchers typically used a U-shape architecture network to predict rainfall (Gao et al. 2022; Xu et al. 2021). This was an interesting and meaningful attempt in the precipitation nowcasting task. However, due to the blurry predictions from the U-shape architecture network, researchers began using the generative adversarial network (GAN) model to obtain more realistic rainfall predictions (Tian et al. 2019). Recently, due to issues with mode

*Corresponding Author

collapse and training instabilities in GAN models (Gao et al. 2024), researchers have applied diffusion models (DMs) for better rainfall prediction (Asperti et al. 2023).

However, the TC precipitation forecasting task does not attract much attention from researchers, which is also important for people to defend against related disasters. Additionally, there are differences between TC precipitation forecasting and regular precipitation forecasting. For example, regular precipitation forecasting usually focuses on a specific fixed region, where the area being predicted does not move with the rainfall. In contrast, in TC precipitation forecasting, the primary region of interest moves with the TC. Therefore, it is inappropriate to directly apply methods designed for regular precipitation forecasting to TC rainfall prediction. A framework specifically designed for TC precipitation is necessary.

Three aspects could be considered: changing the training goal, extracting richer meteorological information from related TC data, and integrating it with NWP.

Changing the training goal: most precipitation forecasting methods predict the absolute value of rainfall. However, future rainfall can be understood as the sum of the current rainfall and change in rainfall (Δ Rainfall) over time. Specifically:

$$Rainfall_{Future} = Rainfall_{Current} + \Delta Rainfall \quad (1)$$

We can train a DL model to predict Δ Rainfall and use Equation 1 to obtain the absolute value of future rainfall, rather than predicting the absolute value of future rainfall directly. This mechanism is advantageous because predicting the change in TC rainfall helps reduce cumulative errors and ensures physical consistency. We define this capability of a model as change awareness. Similar mechanisms are used in some NWP methods to improve the accuracy and stability of meteorological forecasts (Kalnay 2003). Therefore, it is worth considering this mechanism in the TC rainfall prediction task.

Extracting richer meteorological information: most previous DL precipitation forecasting methods attempt to extract sufficient information solely from the rainfall value data. However, the information in rainfall data alone is not adequate for DL models to learn the patterns of TC rainfall. Various TC-related data can help people and DL models understand and predict the tendency of TC rainfall, shown in the red box in Figure 1. For example, rainfall is driven by wind, so the distribution of TC wind is important for TC rainfall prediction. Therefore, in addition to directly extracting information from rainfall data, it is also important to focus on the information derived from the relationships between meteorological factors.

Integrating with NWP models: researchers are trending towards building a suitable “bridge” between DL models and NWP models. Research on this “bridge” can be broadly divided into two categories: 1. using DL methods to replace a part of or all NWP processes (Bi et al. 2023), and 2. focusing on correcting the predictions provided by NWP models (Harris et al. 2022; Zhu et al. 2022). The first category uses the power of DL models’ nonlinear modeling to replace the complex processes of NWP models, making the

prediction process easier and more effective. Methods in this category can learn from historical data, such as TC rainfall data from the past few hours. Models in the second category can more directly extract useful information from prediction results calculated by physical and mathematical equations. Therefore, considering the advantages of both categories, it is beneficial to build a framework that can extract information from various historical variables while also using specific information from NWP results to guide better predictions (Antonio et al. 2024).

Based on these above potentially useful ideas, we propose TCP-Diffusion, a multi-modal diffusion model for global tropical cyclone precipitation forecasting with change awareness. The contributions are summarized as follows:

- TCP-Diffusion can extract information from a rich set of meteorological variables, learn the rules of TC rainfall development, and make skilful predictions for global tropical cyclones. To our knowledge, it is the first global TC precipitation forecasting work based on DL.
- Adjacent Residual Prediction (ARP) is proposed to make our model focus on the rainfall change between adjacent time steps and have the capability of rainfall change awareness. This mechanism can reduce cumulative errors and ensure physical consistency, making the results more realistic and accurate.
- A multi-modal framework is built with several encoder modules to extract extensive information from various meteorological historical data and future predictions provided by NWP. This framework can represent the TC rainfall more comprehensively and provide a “bridge” between DL models and NWP models.
- We show that our model achieves the best performance compared to state-of-the-art (SOTA) DL precipitation forecasting methods and outperforms NWP methods from authoritative meteorological agencies like ECMWF.

Task Definition

Different from regular precipitation forecasting, where the predicted regions are fixed, TC precipitation forecasting focuses on the 10° by 10° rainfall field around the TC center, which moves with the TC. We denote the final output of our work as $\hat{Y} = \{\hat{y}_{n+1}, \hat{y}_{n+2}, \dots, \hat{y}_{n+t}, \dots, \hat{y}_{n+m}\}$, where \hat{y}_{n+t} represents the rainfall prediction around the TC center t time steps into the future. Here, n represents the input time steps and m represents the output time steps. The input data we used can be divided into two parts, as shown in the left part of Figure 2: the first part is historical observation data ($X_{historical} = \{X_1^h, X_2^h, \dots, X_t^h, \dots, X_n^h\}$), where X_t^h is the input data at the t time step and it includes the rainfall value data, Δ Rainfall, the 2-Dimension environment data, and scalar TC variables, like intensity. The second part is the future prediction data from an NWP system ($X_{future} = \{X_1^f, X_2^f, \dots, X_t^f, \dots, X_m^f\}$), where X_t^f denotes the prediction data at future t time step, which is provided by ECMWF (ECMWF 2017). Overall, imagine a TC developing, just like shown in Figure 1. We obtain all

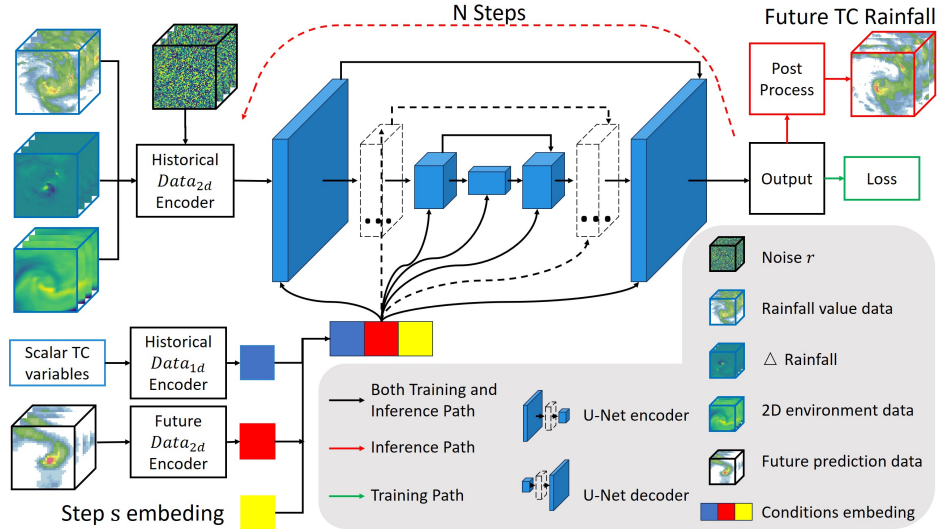


Figure 2: The framework of TCP-Diffusion. U-shape architecture (in the middle) includes the U-Net encoder and U-Net decoder. In inference stage (black+red arrows), the “N Steps” (at the top) means our model will use N loop denoising processes to obtain the result \hat{D}_y and perform Post Process (Equation 1) to get the final predicted TC rainfall \hat{Y} . During the training stage (black+green arrows), “N Steps” and Post Process will not be used. The Output will be used to calculate the loss and update the parameters of TCP-Diffusion.

the input data $X = \{X_{historical}, X_{future}\}$ and then we input them to our model TCP-Diffusion. TCP-Diffusion will extract the TC information from the input data and make a reasonable and accurate rainfall prediction \hat{Y} . We expect \hat{Y} could be as close as possible to the real TC rainfall ($Y = \{y_{n+1}, y_{n+2}, \dots, y_{n+t}, \dots, y_{n+m}\}$) as much as possible, both in the value of the rainfall and the visual authenticity, where y_{n+t} represents the real rainfall around the TC center at the future t time step.

Data

We collected TC various rainfall-related data for our TCP-Diffusion model to comprehensively represent TC rainfall. A total of 1877 TCs spanning from 1980 to 2020 are collected, covering the six major ocean areas. These TC data are divided into three sets: training set (1751 TCs), validation set (87 TCs), and test set (126 TCs from 2018 to 2020). We divided the data into two parts: $X_{historical}$ and X_{future} , which are shown as follows. More details of the data we used could be checked in the **Supplementary Material** and we will also release all these data after that the paper is accepted.

Historical Data

Rainfall Data. It is the main data of this task, denoted as X_{rain} . It is collected from Multi-Source Weighted-Ensemble Precipitation (MSWEP) (Beck et al. 2019), a global precipitation product with a 3-hourly 0.1° resolution available from 1979 to about 3 hours from real-time. We focus only on the rainfall field around the TC center, so we crop and obtain rectangular data covering a 10° by 10° region around the TC center.

Environment Data. Rainfall data provide direct information related to this task, but environmental factors should not be neglected when modeling TC rainfall. Thus, we also collect critical meteorological variables including 2D environment data (ERA5 surface data and ERA5 pressure level data) and Scalar TC variables. The surface data, denoted as X_{SfEnv} , like 2m temperature. ERA5 pressure level data, denoted as X_{PlEnv} , like specific humidity. X_{SfEnv} and X_{PlEnv} are obtained from ERA5 (Hersbach et al. 2020). We perform the same operations as with X_{rain} , focusing on the 10° by 10° region around the TC center. Apart from these above normal environment data, Scalar TC variables are quite related to the TC rain. We consider it as internal environment data, which is denoted as X_{InEnv} . It includes TC intensity, movement velocity, month and the location. X_{InEnv} is collected and calculated from the International Best Track Archive for Climate Stewardship (IBTrACS) resource (Knapp et al. 2010).

Future Prediction Data.

The future prediction data generated by NWP contain explicit physical laws, which are precisely what deep learning methods lack. However, DL models are good at extracting information from data. Therefore, we also consider X_{future} as input data for our model, providing future information and physical laws to some extent. All X_{future} is provided by ERA5-IFS forecasts (ECMWF 2017). There are many variables at the 200 or 850 hPa pressure levels, such as the U-component of wind and the V-component of wind.

Method

TCP-Diffusion is a temporal DM-based method. We call the main component Environment Awareness 3DUNet (EA-3DUNet) (in section EA-3DUNet). As shown in Figure 2,

it can use Historical $Data_{2d}$ Encoder, Historical $Data_{1d}$ Encoders and Future $Data_{2d}$ Encoder to extract TC rainfall information from rainfall related data, 2D environmental factor data, scalar TC variable and future prediction data. 3DUNet is designed to further extract spatiotemporal future from the information provided by different encoders. The inherent power of DMs ensures that the prediction resembles real rainfall data, both in field shape and detail. The information from all the inputs helps the predicted rainfall values closely match the real rainfall data. In the following section, we will introduce the details of TCP-Diffusion. More details of the method could be checked in the **Supplementary Material** and we will also release all these Python codes after that the paper is accepted.

Adjacent Residual Prediction (ARP)

In the TC rainfall forecasting task, predicting the rainfall value directly is difficult because weather systems exhibit chaotic characteristics. Some NWP methods improve the accuracy and stability of forecasts by keeping the weather change as their prediction goal (Kalnay 2003). Inspired by this idea, we find the capability of change awareness is helpful to our model, so we replace the direct prediction of rainfall value with predicting the adjacent residual Δ_x^t between rainfall at adjacent time steps (Δ Rainfall). We call this mechanism Adjacent Residual Prediction. Δ_x^t can be calculated as:

$$\Delta_x^t = X_{rain}^t - X_{rain}^{t-1} \quad (2)$$

where X_{rain}^t and X_{rain}^{t-1} are the original rainfall data at t time step and $t-1$ time step respectively. In our work, apart from the absolute rainfall values data, we add adjacent residual sequence $D_x = \{\Delta_x^1, \Delta_x^2, \dots, \Delta_x^t, \dots, \Delta_x^n\}$, where Δ_x^t is calculated by the Equation 2, which shown as the Δ Rainfall in Figure 2. Additionally, the direct output sequence of our DL model is $\hat{D}_y = \{\hat{\Delta}_y^{n+1}, \hat{\Delta}_y^{n+2}, \dots, \hat{\Delta}_y^{n+t}, \dots, \hat{\Delta}_y^{n+m}\}$, where $\hat{\Delta}_y^{n+t}$ is the adjacent residual we predict between rainfall of time step $n+t-1$ and $n+t$. The final prediction $\hat{Y} = \{\hat{y}_{n+1}, \hat{y}_{n+2}, \dots, \hat{y}_{n+t}, \dots, \hat{y}_{n+m}\}$ can be computed as:

$$\hat{y}_{n+t} = X_{rain}^n + \sum_{z=1}^t \hat{\Delta}_y^{n+z} \quad (3)$$

\hat{Y} is obtained by the accumulation of the latest historical TC rainfall data X_{rain}^n and the adjacent residual prediction $\hat{\Delta}_y$.

Diffusion Model

The prediction process of DMs involves removing noise from a completely random noise r step by step, shown in Figure 2's N Steps. Based on the DMs' generation process, our training goal is to teach our model to perform accurate denoising based on the specific step s and the given information. Specifically, the training goal is to make the noise \hat{r}_s predicted by our model as close as possible to the noise r_s added to the target at the s -th step, $s \in \{1, 2, \dots, N\}$. N is a hyper-parameter.

DMs typically include two processes: a forward noising process and a reverse denoising process. The forward

process has no trainable parameters, so it does not require training a DL model. According to the training goal mentioned above, we need to obtain the sequence D_y^s , where D_y^s is s -th-step noised real adjacent residual $D_y = \{\Delta_y^{n+1}, \Delta_y^{n+2}, \dots, \Delta_y^{n+t}, \dots, \Delta_y^{n+m}\}$. Follow (Ho et al. 2022), D_y^s could be calculated using a random noise $r_s \sim \mathcal{N}(0, 1)$, step s , and the D_y^0 (the original data without noise). The forward process is defined as follows:

$$D_y^s = \sqrt{\bar{\alpha}_s} D_y^0 + \sqrt{1 - \bar{\alpha}_s} r_s \quad (4)$$

where $\bar{\alpha}_s = \prod_{i=1}^s \alpha_i$, $\alpha_s = 1 - \beta_s$, $\beta_s \in (0, 1)$ is predefined by an incremental variance schedule.

For the denoising process, we build the EA-3DUNet, which is defined as follows:

$$\hat{r}_s = EA3DUNet(X_{history}, X_{future}, D_y^s, s, r) \quad (5)$$

where r is the added random noise, $EA3DUNet$ is the trainable model, and \hat{r}_s is the predicted noise. Thus, our training goal can be defined as:

$$L(\theta) = \|r_s - \hat{r}_s\|_2 \quad (6)$$

where θ represents all the trainable parameters in our model. r_s could be calculated by Equation 4.

For the inference phase, we consider a random noise r as the D_y^N (Ho, Jain, and Abbeel 2020) and use the following Equation 7 to denoise D_y^N step by step to obtain the \hat{D}_y^0 , which is equivalent to \hat{D}_y :

$$D_y^{s-1} = \frac{1}{\sqrt{\alpha_s}} (D_y^s - \frac{\beta_s}{\sqrt{1 - \bar{\alpha}_s}} \hat{r}_s) + \sigma_s \epsilon \quad (7)$$

where \hat{r}_s is the predicted noise added at s -th step, σ_s is a variance hyperparameter. $\epsilon \sim \mathcal{N}(0, 1)$ is a random noise, which plays a critical role in generating high-quality prediction in the inference phase (Ho, Jain, and Abbeel 2020).

Environment Awareness 3DUNet (EA-3DUNet)

EA-3DUNet is the main component of TCP-Diffusion. It can extract various features from multi-modal data sources. Due to the differing characteristics and dimensions of these heterogeneous meteorological data, we need to build multiple encoders to embed these data. Therefore, we build the **Historical Data Encoder** for Rainfall Data and Environment Data, and the **Future Prediction Data Encoder** for ECMWF's Future prediction data encoding. To better extract temporal and spatial information from these data, we build **3DUNet** with a temporal and spatial attention mechanism. We will introduce all these modules in the following sections.

Historical Data Encoder. Rainfall Data X_{rain} , adjacent residual data D_x , ERA5 surface data X_{SfEnv} , and ERA5 pressure level data X_{PlEnv} are two-dimensional (2D) data. Considering that our data has a time dimension, we build Historical $Data_{2d}$ Encoder with 3D Convolutional Neural Networks (CNNs) to encode all 2D data with time information first. To reduce computational resources, we use one module to encode these data, so we concatenate them to get

$X_{his2D} = [X_{rain}, D_x, X_{SfEnv}, X_{PLEnv}, r_s]$. This process is defined as follows:

$$e_{his2D} = Conv3d(X_{his2D}, W_{his2D}) \quad (8)$$

where W_{his2D} is the parameter of $Conv3d$ (Historical $Data_{2d}$ Encoder). e_{his2D} represents the features encoded from Historical 2D Data X_{his2D} and serves as the initial feature input to 3DUNet for further feature extraction.

The scalar TC variable X_{InEnv} does not have a 2D structure, so we build Historical $Data_{1d}$ Encoder with Multilayer Perceptron (MLP) and Transformer (Vaswani et al. 2017) layers to encode the X_{InEnv} and obtain the time information. The main process is as follows:

$$e_{mlp} = \phi(X_{InEnv}, W_{mlp}) \quad (9)$$

$$e_{his1D} = Transformer(e_{mlp}, W_{atten}) \quad (10)$$

where ϕ is denoted as an MLP module, which is used for getting the features e_{mlp} of different variables. W_{mlp} is the parameter of ϕ . $Transformer$ module is used for obtaining the time information of X_{InEnv} . W_{atten} is the parameter of $Transformer$ and e_{his1D} is the encoding feature of X_{InEnv} at the initial stage of our model.

Future Prediction Data Encoder. Future Prediction Data X_{future} contain future information and some physical rules provided by NWP, which differ from Historical data. It is challenging for a single module to encode these data containing different types of information at the same time (Alzubaidi et al. 2021). Therefore, we build a Future $Data_{2d}$ Encoder to encode these data and try to obtain more specific features. We use a modified Resnet-18 (He et al. 2016) to obtain the vector. The main process of Future $Data_{2d}$ Encoder is as follows:

$$e_{future} = Resnet(X_{future}, W_{res18}) \quad (11)$$

where $Resnet$ is the Resnet-18 model we used, W_{res18} is denoted as the parameters of Resnet-18, and e_{future} is the condition extracted from X_{future} and used for guide our model to make a better prediction.

3DUNet 3DUNet (Çiçek et al. 2016) is the core component of EA-3DUNet and is a classical DL structure for tasks involving 2D data with time information. It usually includes three parts shown in Figure 2: U-Net encoder ($UNet_{en}$), U-Net decoder ($UNet_{de}$), and the bottleneck between encoder and decoder. There are several modules in $UNet_{en}$ and $UNet_{de}$, called $module_{en}$ and $module_{de}$ respectively. In each module, we build different blocks (blue cuboids) to capture features from various aspects.

Specifically, in the encoder module ($module_{en}$), shown as the blue cuboids in $UNet_{en}$ in Figure 2, we stack two CNN blocks, one spatial attention (SA) block, one temporal attention (TA) block, and a down-sampling block. The network progressively performs downsampling by stacking several $module_{en}$. Each $module_{en}$ receives the feature map from the previous module and also the conditions e_{his1D} and e_{future} from the Historical $Data_{1d}$ Encoder and Future $Data_{2d}$ Encoder, respectively. Additionally, step s is also received to inform the model how much noise to remove at

the current stage. We concatenate these conditions to form the final condition $Cond = [e_{his1D}, e_{future}, s]$. The main process of $UNet_{en}$ is as follows:

$$e_{en}^i = \begin{cases} module_{en}^i(e_{his2D}, Cond, W_{en_i}) & \text{if } i = 1, \\ module_{en}^i(e_{en}^{i-1}, Cond, W_{en_i}) & \text{if } i > 1. \end{cases} \quad (12)$$

where $module_{en}^i$ is the depth- i module in $UNet_{en}$, $i \in \{1, 2, \dots, K\}$. K is a hyper-parameter. W_{en_i} is the parameters of the $module_{en}^i$. if $module_{en}^i$ is the first one ($i = 1$), $module_{en}^1$ receives the e_{his2D} from historical data encoder. if $module_{en}^i$ is not the first one ($i > 1$), $module_{en}^i$ receives the e_{en}^{i-1} from $module_{en}^{i-1}$.

The module between $UNet_{en}$ and $UNet_{de}$ is the Bottleneck. The Bottleneck also contains two CNN blocks, one SA block, and one TA block. The main process is as follows:

$$e_{mid} = Bottleneck(e_{en}^K, Cond, W_{neck}) \quad (13)$$

where e_{mid} is the output of the Bottleneck and W_{neck} is the parameter of Bottleneck.

For $UNet_{de}$, its structure is similar to that of $UNet_{en}$. They both include K modules with similar architecture. In $module_{de}$, there are two CNN blocks, one SA block, one TA block and the final up-sampling block. There are also skip connections between $UNet_{en}$ and $UNet_{de}$. Thus, the definition of $UNet_{de}$ is as follows:

$$e_{de}^i = \begin{cases} module_{de}^i(e_{mid}, Cond, e_{en}^i, W_{de_i}) & \text{if } i = K, \\ module_{de}^i(e_{de}^{i+1}, Cond, e_{en}^i, W_{de_i}) & \text{if } i < K. \end{cases} \quad (14)$$

where $module_{de}^i$ is the depth- i module in $UNet_{de}$, $i \in \{K, \dots, 2, 1\}$. W_{de_i} is the parameters of the $module_{de}^i$. if $module_{de}^i$ is the deepest one ($i = K$), $module_{de}^K$ receives the e_{mid} from the Bottleneck. if $module_{de}^i$ is not the deepest one ($i < K$), $module_{de}^i$ receives the e_{de}^{i+1} from $module_{de}^{i+1}$. if $i = 1$, e_{de}^1 is the final output of EA-3DUNet, which means $\hat{r}_s = e_{de}^1$. Then, we could calculate the loss between r_s and \hat{r}_s to optimize the parameters of our model.

Experiments

Evaluation metrics

Equitable Threat Score (ETS) The Equitable Threat Score (ETS) (Gandin and Murphy 1992) is a metric used to evaluate the accuracy of precipitation forecasts. Compared to the more popular metric, the Critical Success Index (CSI) (Schaefer 1990), it considers the effects of random chance, providing a more equitable assessment of a forecast model's performance (Manzato and Jolliffe 2017). The definition of ETS can be checked in **Supplementary Material**.

We use this metric to show the performance for predicting light, medium, and heavy rainfall, setting thresholds 6 mm/3hr (ETS-6), 24 mm/3hr (ETS-24), and 60 mm/3hr (ETS-60) respectively.

Total Precipitation Mean Absolute Error (TP_{MAE}) TP_{MAE} is a critical index for representing the intensity of TC rainfall. We calculate the absolute difference between real TC rainfall Y and the predicted rainfall \hat{Y} , which is denoted as Total Precipitation Mean Absolute Error (TP_{MAE},

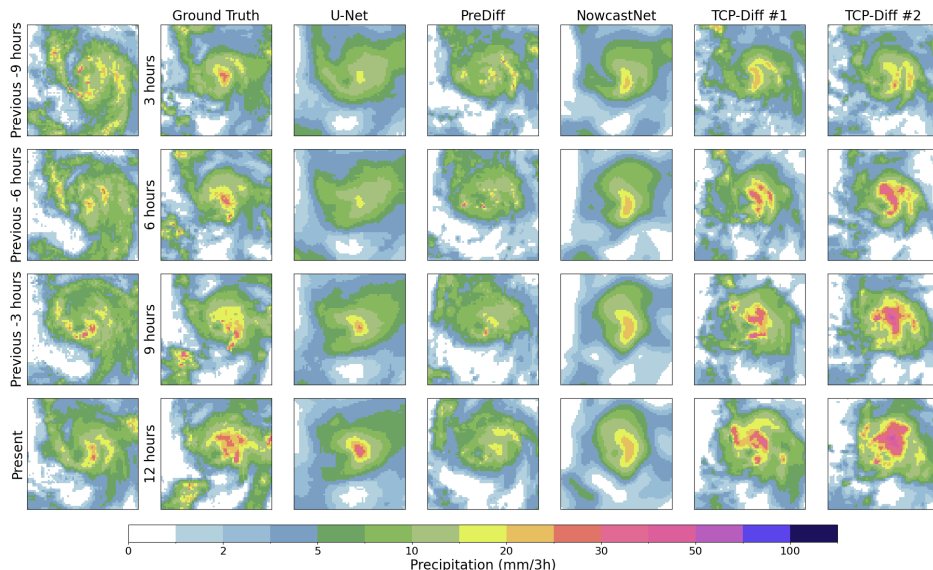


Figure 3: The prediction results of different DL methods on the TC DUMAZILE in North Indian Ocean at 03/03/2018 06:00. The first column is the previous 4 timesteps of rainfall data that is used as input. The second column is the future TC rainfall we want to predict. Each subsequent column from the left shows the predictions from a different DL method. “TCP-Diff #1” and “TCP-Diff #2” are the results from TCP-Diffusion with different initial random noise r .

mm/3hr), to show the prediction skill of different methods at predicting total TC rainfall.

Comparison with State-of-the-art DL Methods

TCP-Diffusion is compared with a deterministic DL method: U-Net (Çiçek et al. 2016). We also compare our model with two generative DL methods developed for now-casting precipitation: PreDiff, which is DM-based (Gao et al. 2024), and NowcastNet (Zhang et al. 2023). We also compare TCP-Diffusion with a basic baseline, persistence forecasting, using the last observed rainfall field for each future prediction (Panofsky 1963).

Qualitative Analysis. Figure 3 shows an example of a single prediction from TCP-Diffusion and comparison DL methods. Comparing the classical rainfall prediction model, like U-Net, the DM-based models (PreDiff and TCP-Diffusion) can give more realistic rainfall predictions with fine spatial detail, such as the shape of the rain band. U-Net and NowcastNet produce predictions that are too spatially smooth. This is one of the reasons we chose DMs as the basis for our TC rainfall prediction model. When comparing our TCP-Diffusion with PreDiff in this example, our model provides more accurate results and does better at predicting the increasing trend of precipitation intensity with time, because the ARP mechanism gives our model the capability to track the rainfall change. We show two samples from TCP-Diffusion, generated using different noise inputs. Overall, they have similar large-scale rainfall trends and structures. This means that the information extracted from other input data, such as historical TC rainfall and 2D environmental variables, can guide our model to make reasonable and realistic forecasts. Overall, TCP-Diffusion can produce rainfall predictions that have realistic spatial and temporal structure, performing better than the other DL methods.

| Model Name | ETS-6 \uparrow | ETS-24 \uparrow | ETS-60 \uparrow | TP _{MAE} \downarrow |
|---------------|------------------|-------------------|-------------------|--------------------------------|
| Persistence | 0.41640 | <u>0.14530</u> | <u>0.00564</u> | <u>0.44558</u> |
| U-Net | 0.44169 | 0.10587 | 0 | 0.47452 |
| PreDiff | 0.38453 | 0.11931 | 0.00430 | 0.53617 |
| NowcastNet | 0.42180 | 0.08990 | 0.00016 | 0.56954 |
| TCP-Diffusion | <u>0.43766</u> | 0.14971 | 0.00742 | 0.42582 |

\uparrow \downarrow Higher is better. Lower is better.

* Bold values are the best. Underlined values are the second best.

Table 1: Comparison with other SOTA DL methods. Equitable Threat Score (ETS) is used to evaluate the prediction skill of each model. ETS-6, ETS-24, and ETS-60 are used to show the prediction skill for light (>6 mm/3hr), medium (>24 mm/3hr), and high (>60 mm/3hr) rainfall respectively. TP_{MAE} shows the total precipitation forecasting skill of different methods and, with unit mm/3hr.

Quantitative Analysis. To further demonstrate the effectiveness of our method, we calculate and compare various metrics of our method with other methods on the entire test set, as shown in Table 1. To ensure the stability and reliability of the results, we randomly select half of the samples from the entire test set, calculate the metrics 10 times, and obtain the mean of these 10 results. For light rainfall prediction (ETS-6), U-Net achieves the best performance, with our method ranking second. However, the performance of U-Net on the other three metrics is unsatisfactory because light rainfall constitutes the majority of TC rainfall. This causes U-Net to focus on the accuracy of light rainfall and neglect the accuracy of moderate and heavy rainfall predictions, which is why it performs well in light rainfall prediction but poorly in heavy rainfall prediction. For higher rainfall thresholds and TP_{MAE}, our method achieves the best performance. Especially in heavy rainfall prediction, TCP-Diffusion shows significant improvement compared to other DL models. It is also the only model to perform better than Persistence forecasting, indicating the value of designing a

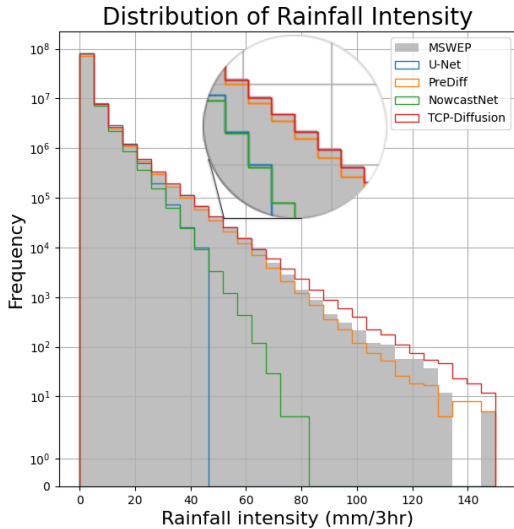


Figure 4: TC rainfall forecasting distributions of different DL methods. The grey histogram is the distribution of MSWEP observations. The coloured lines show histograms of rainfall rates from different DL forecasting methods. The circular magnified region more clearly shows differences between these methods in the high-frequency span of rainfall intensity. Note the logarithmic vertical axis.

| Model Name | ETS-6 \uparrow | ETS-24 \uparrow | ETS-60 \uparrow | TP _{MAE} \downarrow |
|---------------|------------------|-------------------|-------------------|--------------------------------|
| ECMWF-IFS | 0.30193 | 0.08348 | 0.00255 | 0.50661 |
| TCP-Diffusion | 0.41462 | 0.13029 | 0.00551 | 0.47583 |

Table 2: Comparison with NWP methods. The results of ECMWF-IFS are provided by the TIGGE dataset.

specialised system for the task of TC rainfall prediction.

Analysis of TC Rainfall Frequency Distribution. Figure 4 shows histograms of rainfall rates for observations and forecasts by each DL method. We find that the performance of DM-based models, PreDiff and TCP-Diffusion, is much better than that of non-DM-based models, especially in producing a realistic frequency of the heaviest rainfall rates. Our method predicts a slightly higher frequency of the heaviest precipitation intensities than is observed, while PreDiff predicts a slightly lower precipitation intensity. However, for more moderate rainfall intensities, TCP-Diffusion has a more realistic frequency than PreDiff, as shown in the circled region in Figure 4.

Comparison with NWP Methods

We also compare our model with a NWP method. We select the precipitation forecast data in TIGGE provided by ECMWF (ECMWF 2006), denoted as ECMWF-IFS, which performs much better than the ERA5-IFS used in our training stage. However, the spatial resolution of ERA5-IFS is lower than that of ECMWF-IFS, which can save the costs of training. As ECMWF-IFS forecasts in the TIGGE archive are for 6-hourly rather than 3-hourly precipitation, we sum 3-hourly TCP-Diffusion forecasts within each 6-hour interval. Additionally, ECMWF-IFS forecasts start at 12 am and 12 pm UTC each day, so we use TCP-Diffusion to forecast TC rainfall at the same start times. Thus, the test samples in

| ARP | M | F | ETS-6 \uparrow | ETS-24 \uparrow | ETS-60 \uparrow | TP _{MAE} \downarrow |
|--------------|--------------|--------------|------------------|-------------------|-------------------|--------------------------------|
| | | | 0.39109 | 0.12474 | 0.00453 | 0.50109 |
| \checkmark | | | 0.40634 | 0.13014 | 0.00521 | 0.50043 |
| \checkmark | \checkmark | | 0.42926 | 0.14253 | 0.00589 | 0.44632 |
| \checkmark | \checkmark | \checkmark | 0.43766 | 0.14971 | 0.00742 | 0.42582 |

Table 3: Ablation studies. **ARP** means the contribution that we change the regular rainfall value prediction to the adjacent residual prediction. **M** means we not only consider the information from TC rainfall but also consider the TC-related environment information extracted from multi-modal meteorological data. **F** means we combine our DL model with the NWP method by using the predictions provided by NWP to guide the prediction process of our method.

this table are different from those in Table 1.

As shown in Table 2, our method achieves better in all rainfall thresholds ETS and TP_{MAE} than the ECMWF-IFS. This means that low-cost, low-quality NWP methods (ERA5-IFS), when augmented by DL techniques, have the potential to surpass the performance of high-cost, high-quality NWP approaches (ECMWF-IFS).

Ablation Studies

To demonstrate the effectiveness of individual components of our model, an ablation study is conducted. As shown in Table 3, comparing the results from the model with and without **ARP** in the first two rows, we find that changing the regular rainfall value prediction to the adjacent residual prediction results in an improvement in ETS of about 0.1–15.0%. This indicates that predicting the adjacent residual reduces cumulative errors. Then, due to the rich and important TC environment information from multi-modal meteorological data, the model with **M** and **ARP** (third row) performs better than the model with only **ARP**, showing an improvement of about 5.6–13.0% in ETS and a reduction in TP_{MAE}. This demonstrates the significance of building different encoder modules to extract TC rainfall-related information, addressing the deficiency of information provided only by the TC rainfall field. Finally, our complete model TCP-Diffusion including NWP forecast inputs (fourth row) achieves a 1.9–25.9% improvement in ETS over the model with only **M** and **ARP**. This demonstrates that using forecasts provided by NWP to guide DL prediction can enhance skill. Overall, due to the contributions of **ARP**, **M**, and **F**, our final model TCP-Diffusion achieves an improvement in ETS scores of about 11.9–63.8% over the baseline original video diffusion model across the different metrics.

Conclusion

In this paper, we propose TCP-Diffusion for global TC precipitation forecasting, conditional on various meteorological variables. Due to the ARP mechanism, TCP-Diffusion possesses the capability to detect changes in rainfall. Besides, TCP-Diffusion includes a framework with different encoders to extract information from various variables, such as historical TC rainfall data, TC-related environmental data, and forecasting data from NWP models, to guide and control our model for better predictions. TCP-Diffusion produces precipitation predictions in the region around TCs with real-

istic spatial variability and achieves higher skill scores than existing rainfall forecasting methods. It also achieves higher skill scores than a leading NWP system, the ECMWF IFS. In the future, our model can be applied as a component of a forecasting system that includes track and intensity forecasts to produce overall predictions of TC.

References

- Alzubaidi, L.; Zhang, J.; Humaidi, A. J.; Al-Dujaili, A.; Duan, Y.; Al-Shamma, O.; Santamaría, J.; Fadhel, M. A.; Al-Amidie, M.; and Farhan, L. 2021. Review of deep learning: concepts, CNN architectures, challenges, applications, future directions. *Journal of big Data*, 8: 1–74.
- Antonio, B.; McRae, A. T.; MacLeod, D.; Cooper, F. C.; Marsham, J.; Aitchison, L.; Palmer, T. N.; and Watson, P. A. 2024. Postprocessing East African rainfall forecasts using a generative machine learning model. *ESS Open Archive*.
- Asperti, A.; Merizzi, F.; Paparella, A.; Pedrazzi, G.; Angelinelli, M.; and Colamonaco, S. 2023. Precipitation nowcasting with generative diffusion models. *arXiv preprint arXiv:2308.06733*.
- Bai, C.; Sun, F.; Zhang, J.; Song, Y.; and Chen, S. 2022. Rainformer: Features Extraction Balanced Network for Radar-Based Precipitation Nowcasting. *IEEE Geoscience and Remote Sensing Letters*, 19: 1–5.
- Bai, W.; Deng, N.; Sun, Y.; Du, Q.; Xia, J.; Wang, X.; Meng, X.; Zhao, D.; Liu, C.; Tan, G.; et al. 2020. Applications of GNSS-RO to numerical weather prediction and tropical cyclone forecast. *Atmosphere*, 11(11): 1204.
- Beck, H. E.; Wood, E. F.; Pan, M.; Fisher, C. K.; Miralles, D. G.; Van Dijk, A. I.; McVicar, T. R.; and Adler, R. F. 2019. MSWEP V2 global 3-hourly 0.1 precipitation: methodology and quantitative assessment. *Bulletin of the American Meteorological Society*, 100(3): 473–500.
- Benjamin, S. G.; Brown, J. M.; Brunet, G.; Lynch, P.; Saito, K.; and Schlatter, T. W. 2018. 100 Years of Progress in Forecasting and NWP Applications. *Meteorological Monographs*, 59: 13.1 – 13.67.
- Bi, K.; Xie, L.; Zhang, H.; Chen, X.; Gu, X.; and Tian, Q. 2023. Accurate medium-range global weather forecasting with 3D neural networks. *Nature*, 619(7970): 533–538.
- Çiçek, Ö.; Abdulkadir, A.; Lienkamp, S. S.; Brox, T.; and Ronneberger, O. 2016. 3D U-Net: learning dense volumetric segmentation from sparse annotation. In *Medical Image Computing and Computer-Assisted Intervention—MICCAI 2016: 19th International Conference, Athens, Greece, October 17–21, 2016, Proceedings, Part II 19*, 424–432. Springer.
- ECMWF. 2006. TIGGE data available from the ECMWF Data Server. <https://apps.ecmwf.int/datasets/data/tigge/>. Accessed: 2024-07-24.
- ECMWF. 2017. ERA5: Fifth generation of ECMWF atmospheric reanalyses of the global climate. <https://cds.climate.copernicus.eu/cdsapp#!/home>. Accessed: 2024-07-24.
- Gandin, L. S.; and Murphy, A. H. 1992. Equitable skill scores for categorical forecasts. *Monthly weather review*, 120(2): 361–370.
- Gao, Z.; Shi, X.; Han, B.; Wang, H.; Jin, X.; Maddix, D.; Zhu, Y.; Li, M.; and Wang, Y. B. 2024. Prediff: Precipitation nowcasting with latent diffusion models. *Advances in Neural Information Processing Systems*, 36.
- Gao, Z.; Shi, X.; Wang, H.; Zhu, Y.; Wang, Y. B.; Li, M.; and Yeung, D.-Y. 2022. Earthformer: Exploring space-time transformers for earth system forecasting. *Advances in Neural Information Processing Systems*, 35: 25390–25403.
- Harris, L.; McRae, A. T.; Chantry, M.; Dueben, P. D.; and Palmer, T. N. 2022. A generative deep learning approach to stochastic downscaling of precipitation forecasts. *Journal of Advances in Modeling Earth Systems*, 14(10): e2022MS003120.
- He, K.; Zhang, X.; Ren, S.; and Sun, J. 2016. Deep residual learning for image recognition. In *Proceedings of the IEEE conference on computer vision and pattern recognition*, 770–778.
- Hersbach, H.; Bell, B.; Berrisford, P.; Hirahara, S.; Horányi, A.; Muñoz-Sabater, J.; Nicolas, J.; Peubey, C.; Radu, R.; Schepers, D.; et al. 2020. The ERA5 global reanalysis. *Quarterly Journal of the Royal Meteorological Society*, 146(730): 1999–2049.
- Ho, J.; Jain, A.; and Abbeel, P. 2020. Denoising diffusion probabilistic models. *Advances in neural information processing systems*, 33: 6840–6851.
- Ho, J.; Salimans, T.; Gritsenko, A.; Chan, W.; Norouzi, M.; and Fleet, D. J. 2022. Video diffusion models. *Advances in Neural Information Processing Systems*, 35: 8633–8646.
- Huang, C.; Bai, C.; Chan, S.; and Zhang, J. 2022. MMSTN: A Multi-Modal Spatial-Temporal Network for Tropical Cyclone Short-Term Prediction. *Geophysical Research Letters*, 49(4): e2021GL096898.
- Huang, C.; Bai, C.; Chan, S.; Zhang, J.; and Wu, Y. 2023. MGTCF: multi-generator tropical cyclone forecasting with heterogeneous meteorological data. In *Proceedings of the AAAI Conference on Artificial Intelligence*, volume 37, 5096–5104.
- Kalnay, E. 2003. *Atmospheric modeling, data assimilation and predictability*. Cambridge university press.
- Knapp, K. R.; Kruk, M. C.; Levinson, D. H.; Diamond, H. J.; and Neumann, C. J. 2010. The international best track archive for climate stewardship (IBTrACS) unifying tropical cyclone data. *Bulletin of the American Meteorological Society*, 91(3): 363–376.
- Lam, R.; Sanchez-Gonzalez, A.; Willson, M.; Wirnsberger, P.; Fortunato, M.; Alet, F.; Ravuri, S.; Ewalds, T.; Eaton-Rosen, Z.; Hu, W.; et al. 2023. Learning skillful medium-range global weather forecasting. *Science*, 382(6677): 1416–1421.
- Manzato, A.; and Jolliffe, I. 2017. Behaviour of verification measures for deterministic binary forecasts with respect to random changes and thresholding. *Quarterly Journal of the Royal Meteorological Society*, 143(705): 1903–1915.
- Panofsky, H. A. 1963. Determination of stress from wind and temperature measurements. *Quarterly Journal of the Royal Meteorological Society*, 89(379): 85–94.

- Schaefer, J. T. 1990. The critical success index as an indicator of warning skill. *Weather and forecasting*, 5(4): 570–575.
- Tian, L.; Li, X.; Ye, Y.; Xie, P.; and Li, Y. 2019. A generative adversarial gated recurrent unit model for precipitation nowcasting. *IEEE Geoscience and Remote Sensing Letters*, 17(4): 601–605.
- Vaswani, A.; Shazeer, N.; Parmar, N.; Uszkoreit, J.; Jones, L.; Gomez, A. N.; Kaiser, L. u.; and Polosukhin, I. 2017. Attention is All you Need. In Guyon, I.; Luxburg, U. V.; Bengio, S.; Wallach, H.; Fergus, R.; Vishwanathan, S.; and Garnett, R., eds., *Advances in Neural Information Processing Systems*, volume 30. Curran Associates, Inc.
- Vosper, E.; Watson, P.; Harris, L.; McRae, A.; Santos-Rodriguez, R.; Aitchison, L.; and Mitchell, D. 2023. Deep learning for downscaling tropical cyclone rainfall to hazard-relevant spatial scales. *Journal of Geophysical Research: Atmospheres*, 128(10): e2022JD038163.
- Wendler-Bosco, V.; and Nicholson, C. 2022. Modeling the economic impact of incoming tropical cyclones using machine learning. *Natural Hazards*, 110(1): 487–518.
- Xu, F.; Li, G.; Du, Y.; Chen, Z.; and Lu, Y. 2021. Multi-layer networks for ensemble precipitation forecasts postprocessing. In *Proceedings of the AAAI Conference on Artificial Intelligence*, volume 35, 14966–14973.
- Xu, Y.; Wu, B.; Hu, S.; and Zhou, T. 2024. Skillful decadal prediction for Northwest Pacific tropical cyclone activity. *Climate Dynamics*, 1–15.
- Zhang, Y.; Long, M.; Chen, K.; Xing, L.; Jin, R.; Jordan, M. I.; and Wang, J. 2023. Skilful nowcasting of extreme precipitation with NowcastNet. *Nature*, 619(7970): 526–532.
- Zhu, Y.; Zhang, R.-H.; Moum, J. N.; Wang, F.; Li, X.; and Li, D. 2022. Physics-informed deep-learning parameterization of ocean vertical mixing improves climate simulations. *National Science Review*, 9(8): nwac044.